Environmental Science
Water Research & Technology

Effects of Residual Disinfectants on the Redox Speciation of Lead (II)/(IV) Minerals in Drinking Water Distribution Systems

Journal:	*Environmental Science: Water Research & Technology*
Manuscript ID	EW-ART-07-2020-000706.R2
Article Type:	Paper

Water Impact Statement

Lead redox chemistry associated with residual disinfectants controls lead release from corrosion scales in drinking water distribution systems. This study acquired an in-depth understanding on the solid-phase transformation kinetics of Pb(II)/Pb(IV) minerals via the oxidation of free chlorine and bromine. Findings from this study is of interest to scientists, engineers and practitioners concerned with mechanisms that affect lead release in drinking water, and its control.

Effects of Residual Disinfectants on the Redox Speciation of Lead(II)/(IV) Minerals in Drinking Water Distribution Systems

Sumant Avasarala[a], John Orta[a], Michael Schaefer[b],

Macon Abernathy[b], Samantha Ying[b], and Haizhou Liu[a*]

[a] Department of Chemical and Environmental Engineering, University of California, Riverside, Riverside, CA 92521 USA

[b] Department of Environmental Sciences, University of California, Riverside, Riverside, CA 92521 USA

*Corresponding author, e-mail: haizhou@engr.ucr.edu,

phone (951) 827-2076, fax (951) 827-5696

Submitted to *Environmental Science: Water Research & Technology*

Themed issue of *Drinking Water Oxidation and Disinfection Processes*

Abstract

This study investigated the reaction kinetics on the oxidative transformation of lead(II) minerals by free chlorine (HOCl) and free bromine (HOBr) in drinking water distribution systems. According to chemical equilibrium predictions, lead(II) carbonate minerals, cerussite $PbCO_{3(s)}$ and hydrocerussite $Pb_3(CO_3)_2(OH)_{2(s)}$, and lead(II) phosphate mineral, chloropyromorphite $Pb_5(PO_4)_3Cl_{(s)}$ are formed in drinking water distribution systems in the absence and presence of phosphate, respectively. X-ray absorption near edge spectroscopy (XANES) data showed that at pH 7 and a 10 mM alkalinity, majority of cerussite and hydrocerussite was oxidized to lead(IV) mineral $PbO_{2(s)}$ within 120 minutes of reaction with chlorine (3:1 Cl_2:Pb(II) molar ratio). In contrast, very little oxidation of chloropyromorphite occurred. Under similar conditions, oxidation of lead(II) carbonate and phosphate minerals by HOBr exhibited a reaction kinetics that was orders of magnitude faster than by HOCl. Their end oxidation products were identified as mainly plattnerite β-$PbO_{2(s)}$ and trace amounts of scrutinyite α-$PbO_{2(s)}$ based on x-ray diffraction (XRD) and extended X-ray absorption fine structure (EXAFS) spectroscopic analysis. A kinetic model was established based on the solid-phase experimental data. The model predicted that in real drinking water distribution systems, it takes 0.6-1.2 years to completely oxidize Pb(II) minerals in the surface layer of corrosion scales to $PbO_{2(s)}$ by HOCl without phosphate, but only 0.1-0.2 years in the presence of bromide (Br^-) due the catalytic effects of HOBr generation. The model also predicts that the addition of phosphate will significantly inhibit Pb(II) mineral oxidation by HOCl, but only modestly effective in the presence of Br^-. This study provides insightful understanding on the effect of residual disinfectant on the oxidation of lead corrosion scales and strategies to prevent lead release from drinking water distribution systems.

Introduction

Lead (Pb) is a toxic metal that retards mental capabilities in children at low exposure doses and causes organ failure at high exposure levels.[1-4] Lead pipes were commonly used in drinking water distribution systems until 1980s, when U.S. congress amended the Safe Drinking Water Act (SDWA) that mandated the use of "lead-free" plumbing fittings and fixtures.[5-6] Despite that, lead-containing plumbing materials such as brass and tin solder are still in use, which release lead upon corrosion in drinking water distribution systems.[7-11] World Health Organization (WHO) and US EPA's lead copper rule (LCR) established 10 and 15 μg/L, respectively, as the maximum contaminant levels for lead in drinking water.[12-13] However, controlling lead release in drinking water is still challenging; any abrupt changes in drinking water chemistry can disrupt the chemical equilibrium of lead corrosion scales in drinking water distribution systems, resulting in disastrous lead release. One example is the 2014-2017 Flint, Michigan, lead crisis, where the absence of phosphate addition upon a switch of water resources resulted in a rapid lead release much above its MCL.[14-15] Similarly, the change of residual disinfectant from free chlorine (HOCl) to chloramine (NH_2Cl) in Washington D.C. during early 2000s released hazardous levels of lead from drinking water distribution systems.[16-17] According to a recent survey conducted by USEPA on 375 water utility systems across 44 states in the US, HOCl is the preferred disinfectant in almost 259 facilities, most of which are concentrated in California, New York, Tennessee, Michigan, Ohio, Colorado, Florida, Illinois, Oregon, Virginia and Wisconsin.[18] Therefore, taking these factors into consideration, there is an increased need to understand the reaction kinetics between HOCl and lead minerals in drinking water distribution systems.

The speciation of lead minerals and associated redox chemistry with residual disinfectants strongly affect lead release in drinking water distribution systems. Lead exists as Pb(II) or

Pb(IV) minerals in corrosion scales. Pb(II) carbonate minerals, cerussite $PbCO_{3(s)}$ and hydrocerussite $Pb_3(CO_3)_2(OH)_{2(s)}$, are commonly formed in drinking water distribution systems at circumneutral pH conditions.[19-26] To reduce lead solubility in equilibrium with Pb(II) minerals, phosphate (PO_4^{3-}) is commonly added to drinking water as a corrosion control strategy. Addition of PO_4^{3-} leads to the formation of Pb(II) phosphate minerals that have much lower solubilities than Pb(II) carbonate minerals, *e.g.*, chloropyromorphite $Pb_5(PO_4)_3Cl_{(s)}$ and hydroxylpyromorphite $Pb_5(PO_4)_3OH_{(s)}$.[27] In drinking water with a high level of hardness, phosphohedyphane $Pb_3Ca_2(PO_4)_3Cl_{(s)}$ can also form.[20, 28-29] In the presence of HOCl as a residual disinfectant, Pb(II) minerals are oxidized to Pb(IV) as $PbO_{2(s)}$,[7, 16, 30-35] and transient intermediate Pb(III) species are generated during the oxidative pathway.[9, 36, 37] Considering the low solubility of $PbO_{2(s)}$, maintaining its predominance and stability in corrosion scales is desirable.[31, 38-39] Prior studies on the formation of $PbO_{2(s)}$ via Pb(II) minerals oxidation quantified the reaction kinetics of Pb(II) oxidation without a direct quantitative understanding of Pb(IV) formation rates.[7, 9, 40] Additionally, morphological changes of platy hexagonal (hydrocerussite) and prismatic (cerussite) Pb(II) carbonate microcrystals to nanocrystals of PbO_2 were also observed during such oxidative transformational reactions.[31] Though the chlorine-based kinetics data provide insights into the redox reactivities of different Pb(II) minerals, there lacks a direct measurement of solid-phase transformation rate from Pb(II) to Pb(IV) minerals induced by disinfectants. This missing knowledge on solid-phase transformation is critical to the understanding of lead corrosion scales and the development of corrosion control strategies.

Furthermore, water chemistry parameters impact the solid transformation of Pb(II) minerals. For example, changes of pH and alkalinity shift the surface speciation and reactivity of Pb(II) minerals,[35] which consequently impacts the rates of $PbO_{2(s)}$ formation.[31, 41] In addition,

adaptation strategies to climate change including water reuse and desalination can pose a challenge to lead control in drinking water distribution systems, especially considering the presence of elevated levels of salinity (including bromide) in these alternative water sources. In the future, bromide levels in drinking water can increase by over an order of magnitude.[42-43] Elevated bromide in drinking water can catalyze HOCl oxidation via the formation of hypobromous acid (HOBr) as an electron shuttle.[44] HOBr then becomes the *de facto* oxidant and induces much higher reaction rates with relevant Pb(II) minerals than HOCl.[45] Therefore, the effect of bromide on the formation rate of Pb(IV) needs to be better understood.

The objectives of this study are to: (1) predict the predominant lead(II) minerals in drinking water distribution systems under different chemical conditions including pH, alkalinity, calcium, chloride and phosphate; (2) examine the oxidative transformation of Pb(II) minerals by residual disinfectant HOCl and directly quantify the mineral phase transformation rates using start-of-the-art synchrotron techniques; (3) investigate the effects of bromide on the oxidative transformation process and Pb(IV) mineral formation rates.

Materials and Methods

Pb(II) oxidation experiments

Lead minerals including $Pb_3(CO_3)_2(OH)_{2(s)}$, $PbCO_{3(s)}$, scrutinyite α-$PbO_{2(s)}$ and plattnerite β-$PbO_{2(s)}$ were purchased from Sigma-Aldrich. Lead(II) phosphate minerals were synthesized using a standard precipitation method, washed with deionized (DI) water, freeze dried and confirmed for its purity using XRD.[46] The precipitates and the purchased solids were then ground and sieved to a nominal size of 105 to 88 μm using mesh sieves. Fresh HOCl solutions

were diluted from a 5% NaOCl stock solution. HOBr solutions were synthesized by adding 10% molar excess NaBr to a HOCl solution and equilibrated for one hour.[47-48]

Experiments on the oxidative transformation of lead(II) minerals were performed in well-mixed 250-mL glass flasks at 22°C in darkness. 5 g/L of lead(II) carbonate or phosphate mineral was mixed with excess HOCl or HOBr at a molar ratio of 1:3 and an alkalinity of 10 mM as $CaCO_3$. The alkalinity was achieved by using sodium carbonate that was procured from fisher scientific. Furthermore, the initial concentration of reactants was chosen to quantify solid phase reaction kinetics, and avoid alteration of redox reaction thermodynamics under drinking water chemical conditions. The solution pH was adjusted to 7±0.5 and maintained by manual addition of 0.5 M $HClO_4$ or 0.5 M NaOH whenever necessary. A pH of 7 was used to represent the redox reactivity with HOCl (pK_a = 7.6) that largely drive the oxidative transformation from Pb(II) to Pb(IV).[31] Samples were taken at pre-determined time intervals and filtered with 0.1-μm filters. Retained solids were washed with 50 mL DI water to remove residual oxidant and freeze dried for subsequent solid phase analysis. Furthermore, anoxic experiments using the above experimental conditions were also conducted on both Pb(II) carbonate and phosphate minerals in a glove box, to monitor dissolved oxygen (DO) release during the oxidation experiments that assisted the reaction mechanism investigation. DO measurements were made using an Orion Star A113 Dissolved Oxygen Benchtop Meter. [HOCl] or [HOBr] concentration, which is the sum of both [OCl^-] and [HOCl] in the filtered samples was analyzed using the standard DPD method.[49]

Solid phase analysis

Solid phase analysis on the filter retained samples was conducted using X-ray absorption spectroscopy (XAS) and X-ray diffraction (XRD) to quantify the speciation and oxidation states

of lead in solid samples. Specifically, XANES and EXAFS spectra were collected to monitor changes in solid fractionation of Pb(II)/Pb(IV) and their mineralogy in solids reacted with HOCl/HOBr. X-ray absorption spectroscopy measurements for Pb-L_{III} edge (13035 eV) were performed at beamlines 11-2 and 4-1 of the Stanford Synchrotron Radiation Lightsource. Prior to spectroscopic analysis, the samples were ground and diluted using boron nitride (BN) to reach an absorption length of 1.5 cm. Measurements were taken from 12800 to 13925 eV (approximately 30 min per scan) to include both XANES and EXAFS regions (to k = 12). The collected spectra were then processed using Athena software[50], where the fraction of different oxidation states and different minerals were obtained by conducting a linear combination fitting (LCF) on XANES and EXAFS data, respectively. The crystal chemistry and minerals in the solid samples were identified using a PANalytical Empyrean Series 2 XRD instrument.

Equilibrium modelling and kinetics modeling

Predominant lead(II) minerals in drinking water distribution systems under different chemical conditions were predicted based on chemical equilibria using the Geochemist's Workbench software.[51] Reaction equilibrium constants were obtained from the Visual MINTEQ database.[52] Additional details of geochemical modelling are provided as Text S1 in the Supplementary Information (SI). Solid phase reaction kinetics of Pb(II) oxidation by chlorine/bromine were modeled using second-order reaction kinetics. Details on the data fitting of the kinetics rate constants were provided in Text S2 of the SI.

Results and Discussion

Effect of alkalinity and phosphate on lead (II) mineral speciation

Chemical equilibrium modelling of drinking water distribution systems using different corrosion control strategies suggested the formation of Pb(II) carbonates (cerussite and hydrocerussite) and phosphates (chloropyromorphite) under relevant conditions (Figure 1). Predominant Pb(II) minerals in the corrosion scales of lead-containing drinking water distribution systems vary greatly based on the drinking water chemistry and implementation of corrosion control strategies. In systems that only use pH or alkalinity adjustments as the corrosion control strategy,[53-56] cerussite and hydrocerussite are the predominant lead(II) minerals (Figure 1a), consistent with observations from prior studies.[31, 57] However, under these conditions, *i.e.*, pH between 7 and 8, and alkalinity between 0 and 100 mg/L as $CaCO_3$, the solubility of lead ranges between 0.1 and 1 mg/L, which is one to two orders of magnitude higher than the World Health Organization's (WHO) international regulatory standard of ≤10μg/L. Another common lead corrosion control strategy in drinking water distribution system is the addition of phosphate,[10, 58] with a typical phosphate concentration of 0.5-2 mg/L. Under these conditions, chemical equilibrium predicts the formation of chloropyromorphite $Pb_5(PO_4)_3Cl_{(s)}$ across all relevant pH conditions (Figure 1b). This is consistent with prior investigations where, the formation of chloropyromorphite was observed to be kinetically favorable across all pH [59], specifically in the presence of commonly observed Pb(II) minerals in corrosion scales, cerussite[31] and hydroxyapatite[60]. The solubility of chloropyromorphite is much lower than either cerussite and hydrocerussite, resulting in an equilibrated soluble Pb level between 0.2 and 10 μg/L that is within the WHO's international regulatory standard of ≤10μg/L. Furthermore, in cases with increasing chloride levels, the solubility of chloropyromorphite continues to drop (Figure S1). Therefore, for distribution systems with a high level of chloride in the water source, adding phosphate minimizes lead solubility and leaching risks.

169 ***Solid-phase transformation kinetics of Pb(II) minerals by HOCl***

170 Transformation of Pb(II) minerals to Pb(IV) solids by HOCl under typical drinking water
171 chemical conditions is thermodynamically favorable, and the experimental conditions chosen for
172 the oxidation experiments did not change the reaction thermodynamics and provided insight into
173 the redox reactivity in actual drinking water systems (Table S1). When cerussite was exposed to
174 chlorine, changes in the XANES spectra (acquired at Pb L_{III} edge) of cerussite with increasing
175 reaction time suggested the oxidative transformation of Pb(II) in $PbCO_{3(s)}$ to Pb(IV). This change
176 was indicated by the formation of pre-edge Pb(IV) shoulder and post-edge Pb(IV) peak at 13030
177 and 13060 eV, respectively (Figure 2a).[61] Linear combination fitting (LCF) of the XANES data
178 showed that the solid phase oxidation of $PbCO_{3(s)}$ followed a *second* order reaction kinetics,
179 where 70% of Pb(II) in $PbCO_{3(s)}$ was converted to Pb(IV) within 120 minute of reaction (Figure
180 2b). The second-order rate constant for this reaction was estimated to be 7.4×10^{-3} $L\bullet m^{-2}\bullet min^{-1}$
181 (Figure 3, S2). Furthermore, results from the LCF fitting the EXAFS data confirmed that the
182 Pb(IV) generated during the oxidative transformation of $PbCO_{3(S)}$ existed as PbO_2 within the
183 solids (Figure S3a, b). This PbO_2 was later confirmed as β-$PbO_{2(s)}$ with a trace amount of
184 scrutinyite α-$PbO_{2(s)}$ using an XRD (Figure S4). These results agree with observations reported
185 in other investigations, where α-PbO_2 and β-PbO_2 were identified as the two corrosion products
186 of $PbCO_{3(s)}$.[20, 31, 40]

187 Similar to cerussite, the XANES spectra of hydrocerussite confirmed the oxidation of Pb(II) to
188 Pb(IV) by HOCl (Figure 2c). Hydrocerussite oxidation also followed *second*-order reaction
189 kinetics, where 90% of Pb(II) was converted to Pb(IV) within 120 minutes, ~20% higher than
190 those observed during cerussite oxidation (Figure 2d, Figure S2c-d). Unlike in the case of
191 cerussite, a lag phase was observed prior to the oxidative transformation of Pb(II) to Pb(IV) with

3.32×10^{-3} $L\bullet m^{-2}\bullet min^{-1}$ as the estimated reaction rate constant (Figure 3, S5). During the lag phase, LCF of the EXAFS data suggested an exponential increase in cerussite percentage from 0% to approximately 30% and eventually dropped to 7% as the reaction proceeded (Figure S3c, d). These XAS results further validate XRD observations made in previous investigations that identified cerussite as an intermediate product of hydrocerussite oxidation using HOCl.[9, 31] In contrast to the lead(II) carbonate minerals, lead(II) phosphate minerals showed much less reactivity with HOCl (Figure S6, S7 and S8). No noticeable oxidation was observed even after 5 days of reaction with HOCl based on XANES and XRD data.

Effects of bromide on the solid-phase transformation kinetics of Pb(II) minerals

Increased bromide concentrations in drinking water distribution systems results in the formation of HOBr from HOCl, which is thermodynamically capable of oxidizing Pb(II) solids to Pb(IV) (Table S1):

$$HOCl + Br^- \rightarrow HOBr + Cl^- \qquad \textit{(Reaction 1)}$$

To evaluate the effects of bromide, we conducted HOBr oxidation experiments on representative Pb(II) carbonate and phosphate minerals. Experimental results and post-experiment XANES analysis on cerussite and hydrocerussite indicated 93% and 96% oxidative transformation of Pb(II) to Pb(IV) within 30 minutes (Figure 4a-d). Oxidative transformation of cerussite was greater with HOBr (93%) than with HOCl (70%) unlike in the case of hydrocerussite where the difference was insignificant. Both reactions (cerussite-HOBr and hydrocerussite-HOBr) followed *second* order reaction kinetics with 5.05×10^{-2} and 1.8×10^{-2} $L\bullet m^{-2}\bullet min^{-1}$ as their estimated reaction constants (Figure 3, S9, S10). These estimated rate constants were almost an order of magnitude greater than those observed with HOCl. Therefore, indicating HOBr as an oxidant

214 with a higher oxidation potential than HOCl, similar to prior observations made in drinking
215 water distribution systems.[45] Analytical results from XRD and EXAFS confirmed that the Pb(IV)
216 formed from both cerussite and hydrocerussite oxidation existed as α-$PbO_{2(s)}$ and β-$PbO_{2(s)}$
217 within the solids (Figure S11 and S12a-d). These results are coherent with observations made
218 during reactions with HOCl.[20, 31, 40]

219 Unlike reaction with HOCl, approximately 13% and 22% of Pb(II) in hydroxylpyromorphite and
220 chloropyromorphite, respectively, were oxidized to $PbO_{2(s)}$ by HOBr in just 420 minutes (Figure
221 5a-d). These results agree with our thermodynamic predictions which suggested a higher
222 susceptibility of pyromorphites to oxidize on reaction with HOBr (Table S1). For the first 120
223 minutes of the reaction, there was negligible oxidation in both pyromorphite(s), however, after
224 120 minutes there was a linear increase in the Pb(IV) fraction (Figure 5a-d). Oxidation of both
225 hydroxylpyromorphite and chloropyromorphite followed *second*-order reaction kinetics, whose
226 reaction rate constants were estimated to be 0.34×10^{-3} $L\bullet m^{-2}\bullet min^{-1}$ and 3.62×10^{-03} $L\bullet m^{-2}\bullet min^{-1}$
227 (Figure 3, S13, S14). Results from EXAFS and XRD analyses indicate that only 13% of
228 hydroxylpyromorphite and 22% of chloropyromorphite were oxidized to form β-$PbO_{2(s)}$ (Figure
229 S15a-d, S16). Chloropyromorphite exhibited a higher oxidation rate than hydroxylpyromorphite.

230 ***Reaction Stoichiometry and Pb(II) mineral oxidation pathway***

231 The molar ratio of the amount of Pb(II) oxidized to the amount of oxidant (HOCl or HOBr),
232 defined as Δ[Pb(II)]/Δ[oxidant] theoretically equals one if electrons only flow between Pb(II)
233 solids and the oxidant. Experimental data showed that this stoichiometric molar ratio was equal
234 to the theoretical value during the oxidation of Pb(II) carbonate minerals by HOCl and HOBr
235 (Figure 6). In contrast, the stoichiometric molar ratio was significantly less than the theoretical
236 prediction for oxidation involving Pb(II) phosphate minerals – the molar ratio was negligible

with HOCl, and ranges between 0.06 and 0.13 with HOBr (Figure 6), indicating other reaction pathways can consume HOCl or HOBr without directly oxidizing Pb(II) phosphate minerals.

Additional oxidation experiments with Pb(II) phosphate minerals under anaerobic conditions showed that dissolved oxygen was generated when HOBr was consumed in comparison to the control (Figure S17). This observation indicates the disproportionation of HOBr into bromide and oxygen, a process that can be catalyzed by Pb intermediates. Prior studies observed short-lived Pb(III) hydroxyl aqua complex intermediates – typically existing as $Pb(OH)_2(H_2O)^{\bullet+}$ and $Pb(OH)_3(H_2O)_2^{\bullet}$ at circumneutral pH ranges – are generated during the rapid hydroxyl radical-driven oxidation of Pb(II).[36-37] Pb(III) intermediates can subsequently disproportionate and withdraw electrons from its hydroxyl groups, thus converting itself back to Pb(II) and generating dissolved oxygen.

Environmental Implications

This study offers findings through a comprehensive examination of solid transformation of lead minerals by residual disinfectants in drinking water distribution systems. Chemical equilibrium simulations suggest that cerussite and hydrocerussite are relevant Pb(II) minerals in the absence of phosphate, whereas chloropyromorphite is the predominant Pb(II) mineral in the presence of phosphate. To further evaluate the importance of bromide on the oxidative transformation of Pb(II) minerals in drinking water distribution systems, a kinetic model was established to predict the time it takes to convert 90% of Pb(II)-containing surface layer of corrosion scales to $PbO_{2(s)}$ (Text S3). The data predict that it takes up 0.6-1.2 years to oxidize 90% of Pb(II) carbonate minerals in drinking water distribution systems with HOCl but only takes 0.1-0.2 years in the presence of trace levels of bromide (Figure 7). In contrast, oxidation is much slower in systems

with phosphate, taking 50-55 years and approximately 1.6-1.8 years to oxidize 90% of Pb(II) phosphate minerals at very low (0.018 mg/L) and high (3.2 mg/L) bromide levels, respectively (Figure 7, Text S3). Oxidation of Pb(II) minerals to $PbO_{2(s)}$ is a desirable lead mitigation strategy considering the low solubility of $PbO_{2(s)}$, although other factors such as the presence of natural organic matter may enhance colloidal mobilization of $PbO_{2(s)}$ particles leading to higher overall lead exposure.[34, 62-63] Further work is needed to investigate the effects of Pb(IV) formation and associated chemistry on the control of lead release.

Conflicts of interest

There are no conflicts of interest to declare.

Acknowledgements

This research was supported by grants to H. Liu from U.S. National Science Foundation CAREER Program (CBET- 1653931) and the University of California Multicampus Research Programs and Initiatives award (MRP-17-455083), and to J.Orta from the Department of Education GAANN Fellowship (P200A180038). We thank Steven Crumly from the University La Verne for participating in this project. M.J. Abernathy was supported by a T32 Training Grant from the National Institute of Health (T32 ES018827). We also thank Ryan Davis, Matthew Latimer, and Erik Nelson for help with data collection at SSRL. Portions of this research were carried out at the Stanford Synchrotron Radiation Lightsource, a Directorate of SLAC National Accelerator Laboratory and an Office of Science User Facility operated for the U.S. Department of Energy Office of Science by Stanford University.

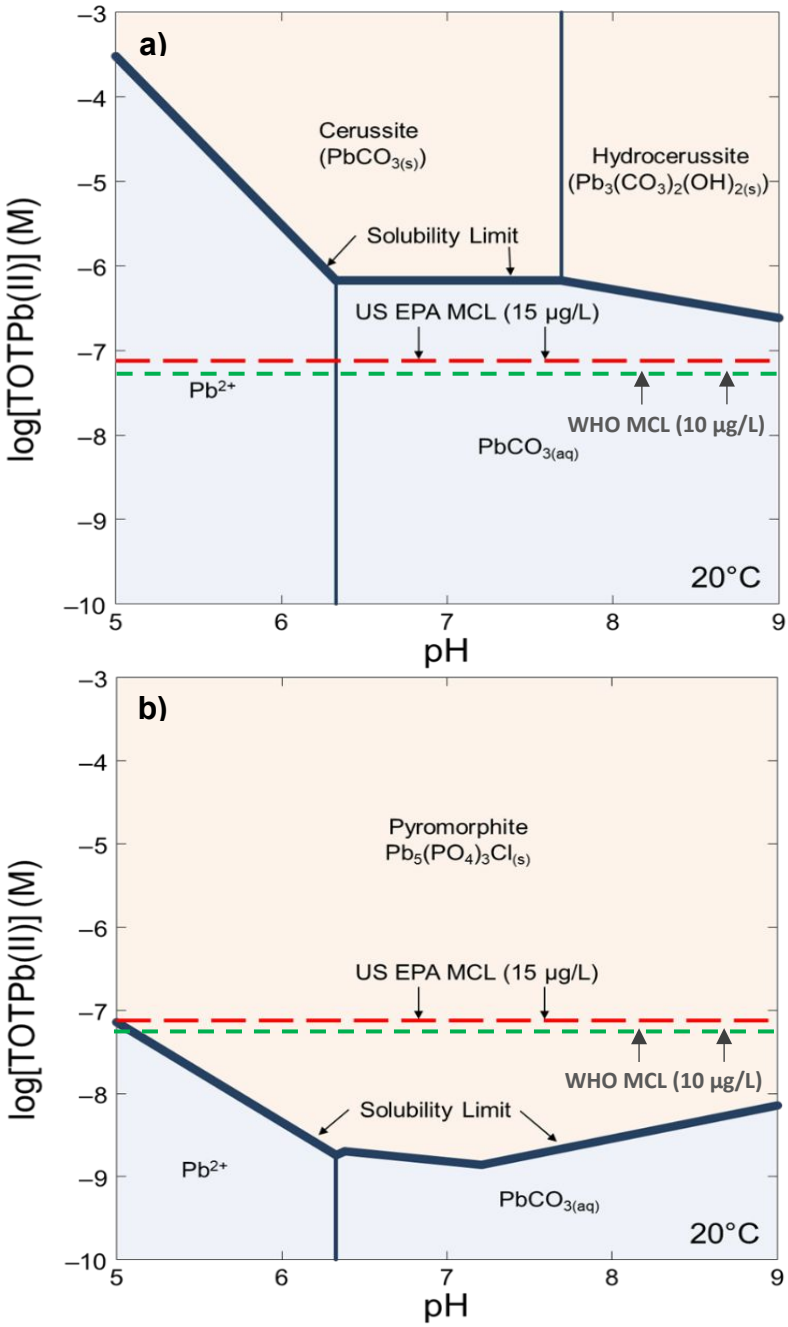

Figure 1 Chemical equilibrium modeling of lead(II) minerals in corrosion scales of drinking water systems utilizing different control strategies. Bolded line represents the total dissolved Pb(II) concentration. Red dashed line represents the USEPA MCL for lead. T=20 °C, green dashed line represents the WHO MCL for lead, ionic strength=0.01 M. **(a)** $TOTCO_3$=1 mM, [Cl^-]=0.1 mM; **(b)** $TOTCO_3$=1 mM, [Cl^-]=0.1 mM, [$PO4^{3-}$] = 0.5 mg/L as PO_4.

285

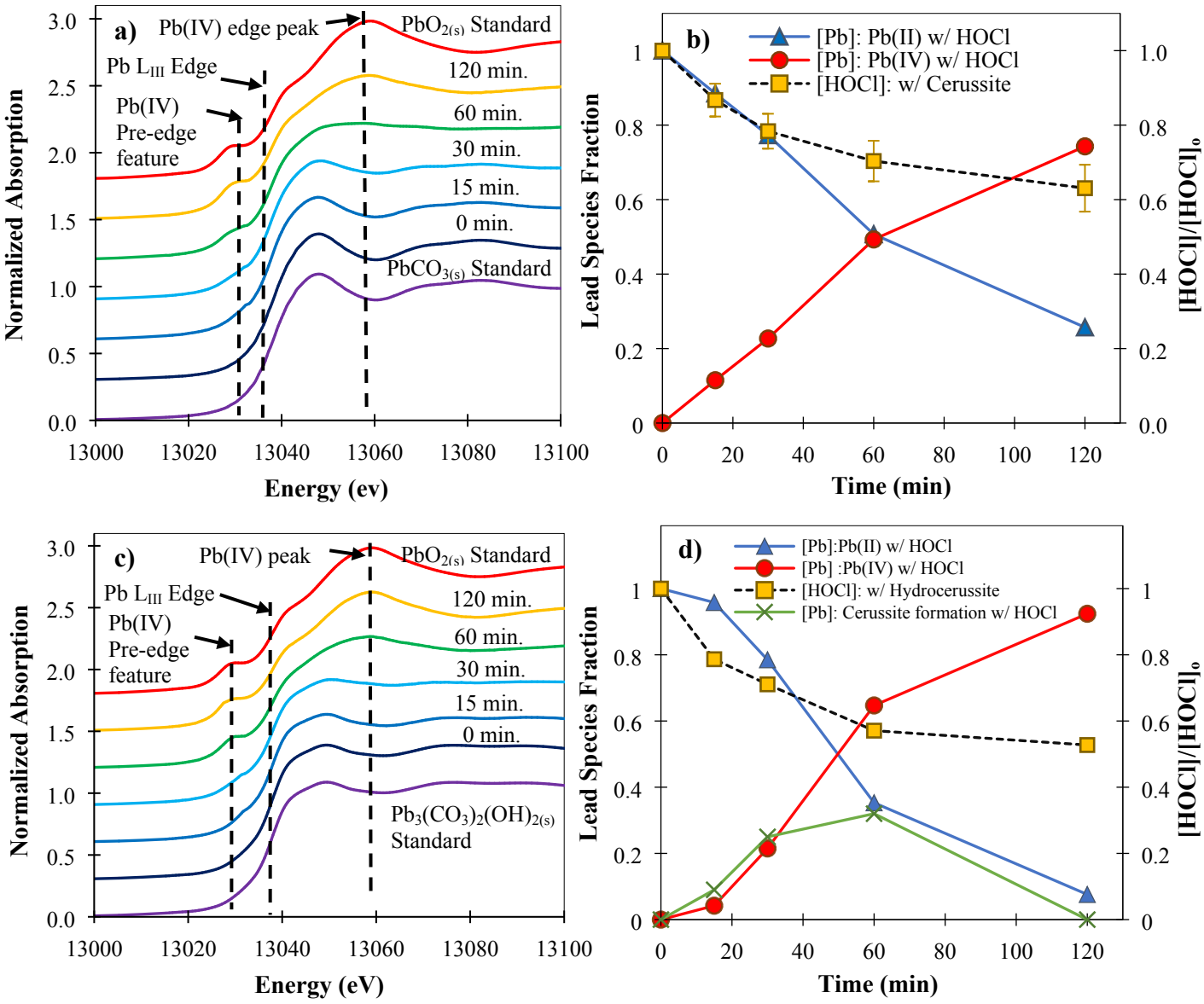

286 **Figure 2** Oxidation of lead(II) carbonate minerals by HOCl to $PbO_{2(s)}$. $TOTCO_3$ = 10 mM,
287 $[HOCl]_0$ = 4.2 g/L as Cl_2, initial Cl_2:Pb(II)=3:1, T=22°C, pH=7 **(a)** XANES of cerussite
288 oxidation; $[PbCO_{3(s)}]_0$ = 5 g/L **(b)** Lead speciation in cerussite oxidation **(c)** XANES
289 hydrocerussite of oxidation; $[Pb_3(CO_3)_2(OH)_{2(s)}]_0$ = 5.0 g/L **(d)** Lead speciation in hydrocerussite
290 oxidation. The black dashed lines in figures a and c represent the pre-edge feature characteristic
291 of Pb(IV), Pb L_{III} edge and Pb(IV) peak, respectively.

292

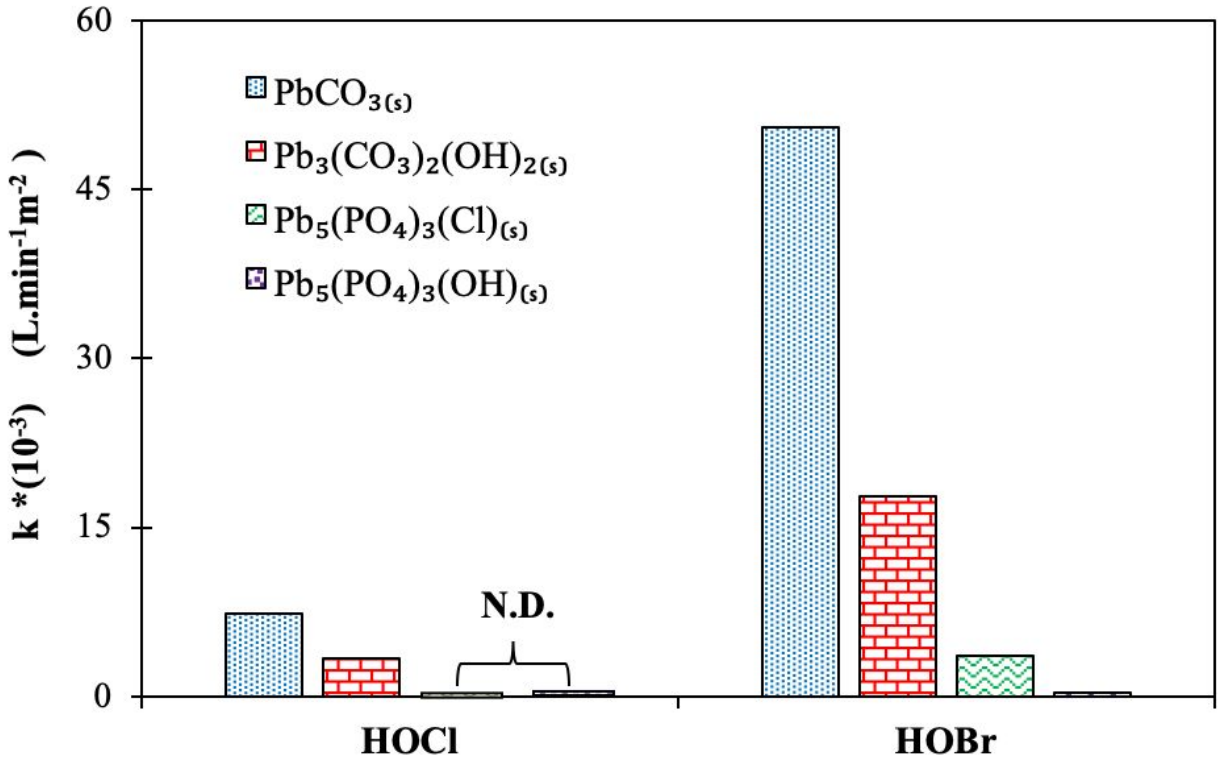

293

294 **Figure 3** Second-order rate constant k ($L \cdot m^{-2} \cdot min^{-1}$) for oxidation of lead(II) minerals using
295 HOCl/HOBr. Reaction rate constants for Pb(II) phosphate minerals reaction with HOCl
296 (represented by blank bars) could not be determined. N.D = Not Detectable

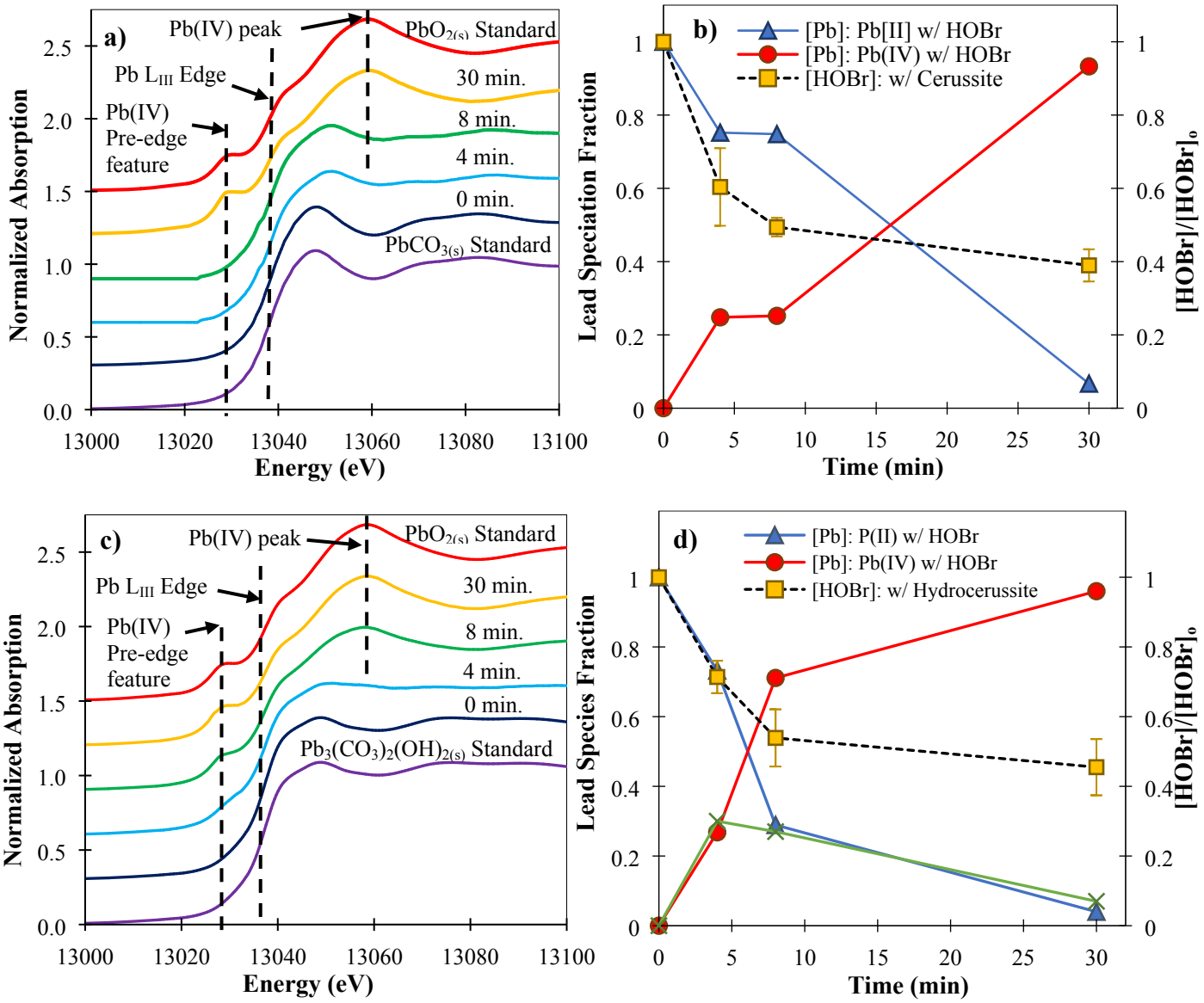

Figure 4 Lead carbonates oxidation by HOBr. $TOTCO_3$ = 10 mM, $[HOBr]_0$ = 4.2 g as Cl_2/L (59.2 mM), initial Cl_2:Pb(II)=3:1, T=22°C, pH=7 **(a)** XANES of cerussite oxidation; $[PbCO_{3(s)}]_0$ = 5 g/L **(b)** Lead speciation in cerussite oxidation **(c)** XANES hydrocerussite of oxidation; $[Pb_3(CO_3)_2(OH)_{2(s)}]_0$ = 5.0 g/L **(d)** Lead speciation in hydrocerussite oxidation. The black dashed lines in figures a and c represent the pre-edge feature characteristic of Pb(IV), Pb L_{III} edge and Pb(IV) peak, respectively.

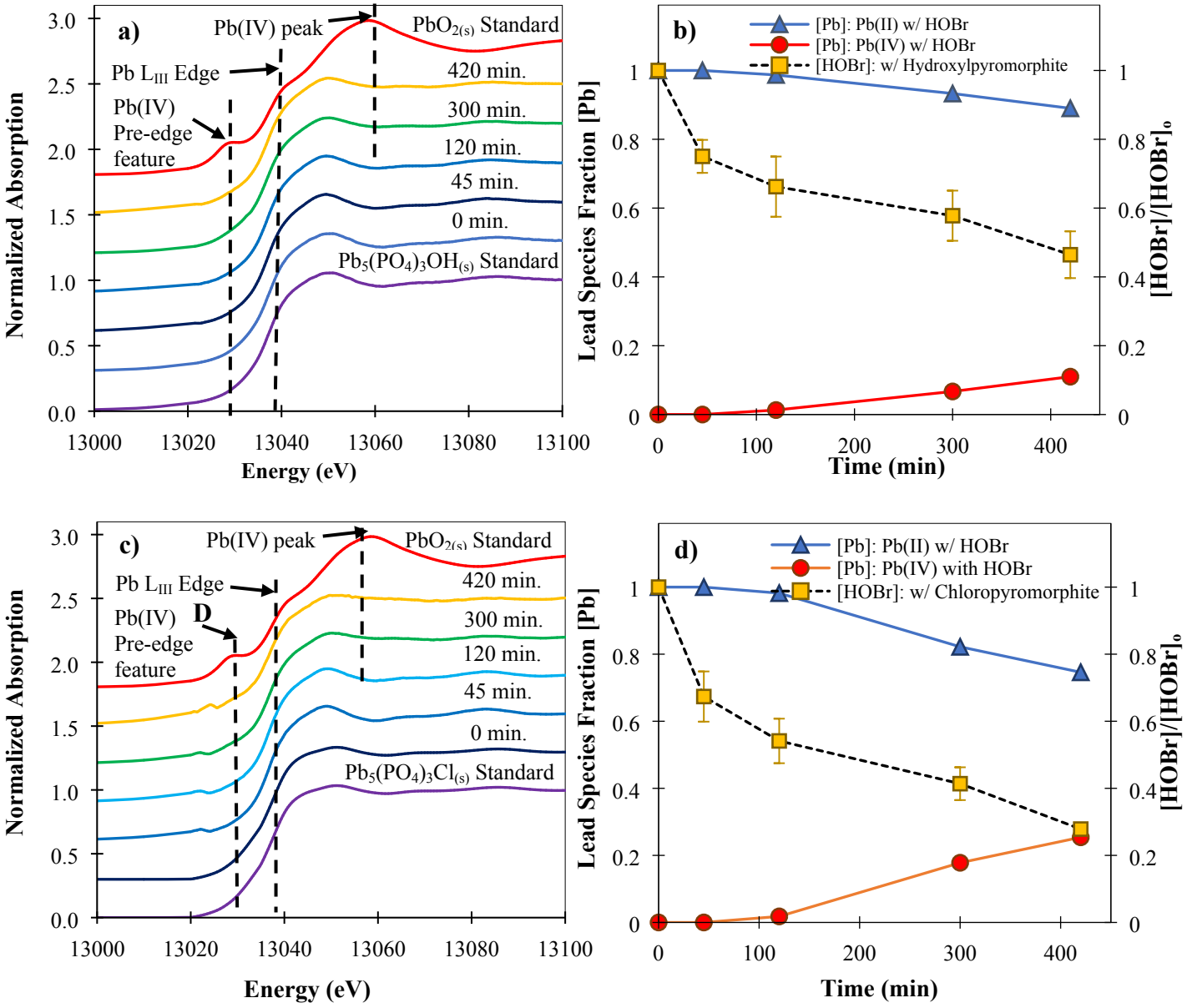

Figure 5: Oxidation of lead(II) phosphate minerals by HOBr. $TOTCO_3$ = 10 mM, $[HOBr]_0$ = 4.2 g as Cl_2/L, initial Cl_2:Pb(II)=3:1, T=22°C, pH=7. **(a)** XANES of hydroxylpyromorphite oxidation; $[Pb_5(PO_4)_3OH_{(s)}]_0$ = 5 g/L **(b)** Lead speciation in hydroxylpyromorphite oxidation. **(c)** XANES of chloropyromorphite oxidation; $[Pb_5(PO_4)_3Cl_{(s)}]_0$ = 5 g/L **(d)** Lead speciation in chloropyromorphite oxidation. The black dashed lines in figures a and c represent the pre-edge feature characteristic of Pb(IV), Pb L_{III} edge and Pb(IV) peak, respectively.

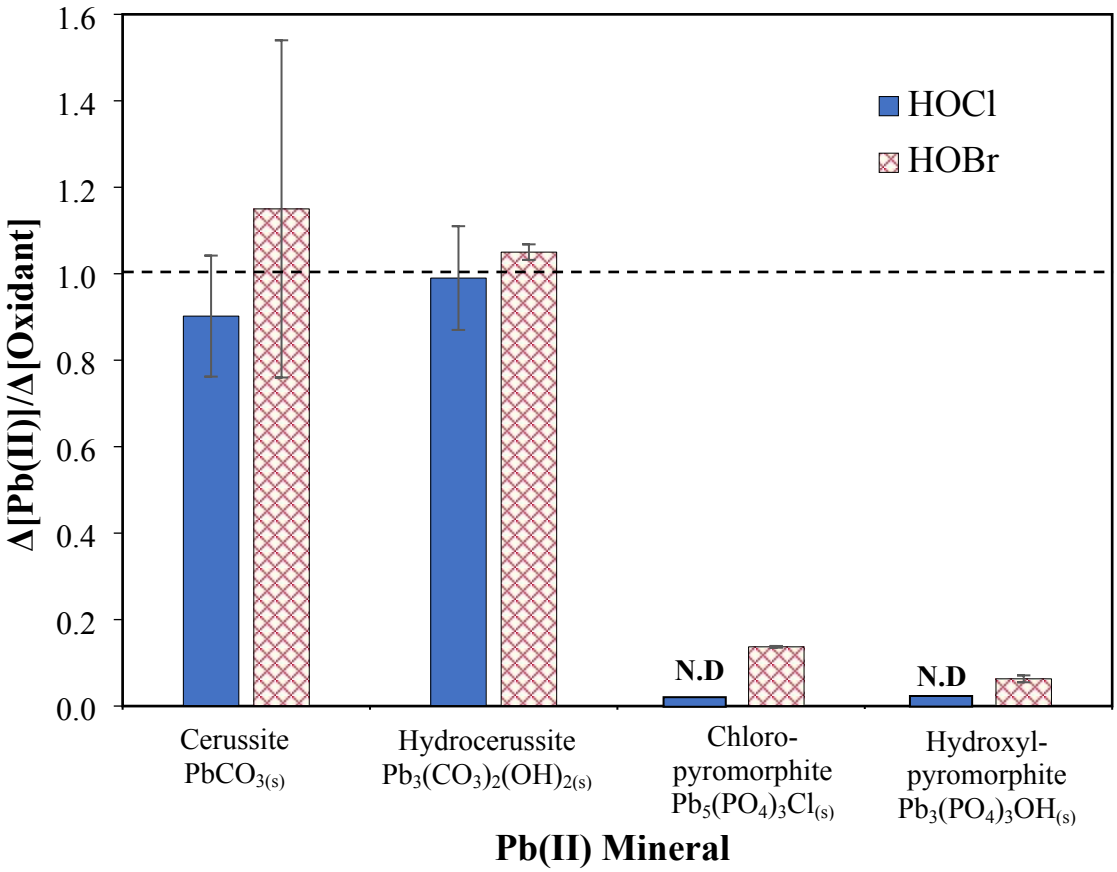

Figure 6 The molar Ratio between consumption of lead(II) mineral and oxidant (Δ[Pb(II)]/Δ[Oxidant]) during reaction with HOCl and HOBr. The ratio for Pb(II) phosphate minerals during reaction with HOCl (represented by blank bars) could not be determined, as Pb(II) consumption was negligible. N.D = Not detectable (no Pb(II) oxidation was observed). Minor deviations from 1 for Pb-carbonate minerals were observed due to non-ideal behavior of the reaction.

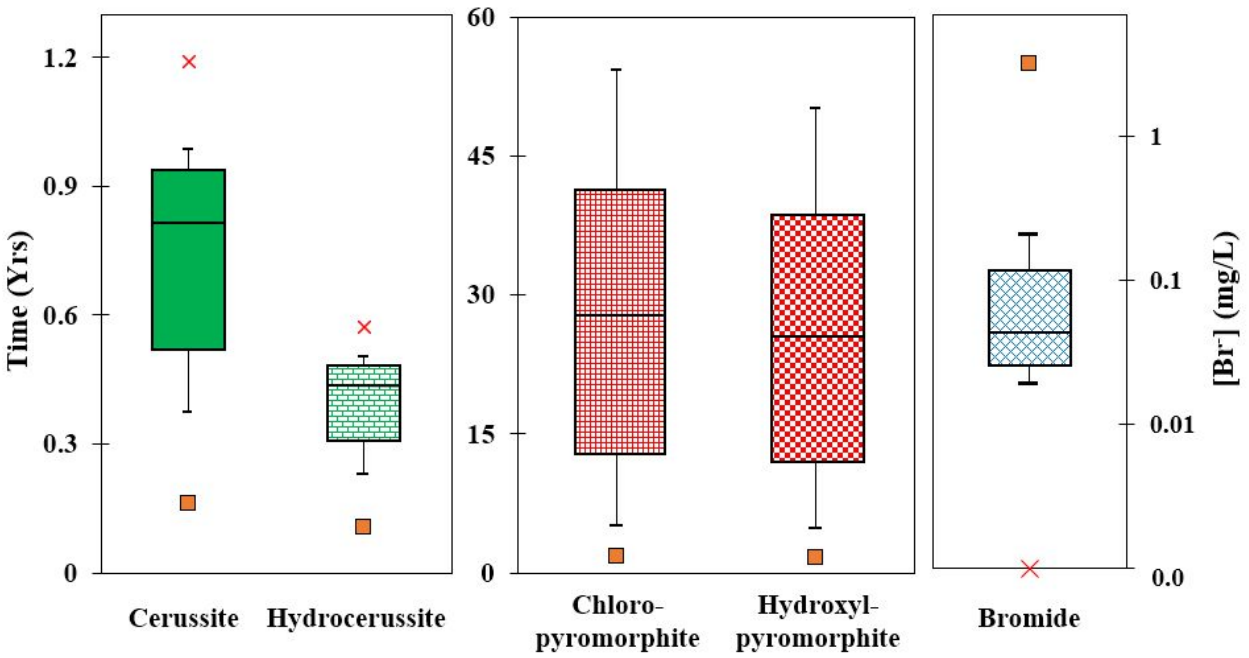

Figure 7 Time required to oxidize 90% of different Pb(II) minerals to Pb(IV) in drinking water distribution systems utilizing HOCl in the presence of varying bromide concentrations pH = 7, T = 22°C, $[Oxidant]_{ss}$ = 0.5 mg/L as Cl_2. Cross and squares markers represent values predicted based on the minimum (0 mg/L) and maximum (3.2 mg/L) bromide concentration, respectively. Whiskers represent predictions based on the 5 percentile and 95 percentile distributions of bromide concentrations. Horizontal lines of the box plot represent predictions based on the 1st, 2nd, and 3rd quartile of bromide concentration distribution.

References

1. Stokes, L. O., N. C.; Thomas, P.; Davies-Cole, J. O, Blood lead levels in residents of homes with elevated lead in tap water. District of Columbia, 2004. *MMWR. Morbidity and mortality weekly report* **2004,** *53* (12), 268.
2. Ferrie, J. P.; Rolf, K.; Troesken, W., Cognitive disparities, lead plumbing, and water chemistry: Prior exposure to water-borne lead and intelligence test scores among World War Two US Army enlistees. *Econ. Hum. Biol.* **2012,** *10* (1), 98-111.
3. Gidlow, D., Lead toxicity. *Occup. Med.* **2004,** *54* (2), 76-81.
4. Abadin, H. A., A.; Stevens, Y.W., Toxicological profile for lead. US Department of Health and Human Services. *Public Health Service. Agency for Toxic Substances and Disease Registry, Atlanta, USA* **1988**.
5. EPA, U. S., Lead Ban: Preventing the Use of Lead in Public Water Systems and Plumbing Used for Drinking Water. National Service Center for Environmental Publications (NSCEP), **1989** https://nepis.epa.gov
6. Calabrese, E. J., Safe Drinking Water Act. CRC Press: **1986**, https://www.epa.gov/sdwa
7. Liu, H.; Korshin, G. V.; Ferguson, J. F., Interactions of Pb(II)/Pb(IV) solid phases with chlorine and their effects on lead release. *Environ. Sci. Technol.* **2009,** *43* (9), 3278-3284.
8. Liu, H.; Schonberger, K. D.; Korshin, G. V.; Ferguson, J. F.; Meyerhofer, P.; Desormeaux, E.; Luckenbach, H., Effects of blending of desalinated water with treated surface drinking water on copper and lead release. *Water Res.* **2010,** *44* (14), 4057-4066.
9. Kim, E. J.; Herrera, J. E., Characteristics of lead corrosion scales formed during drinking water distribution and their potential influence on the release of lead and other contaminants. *Environ. Sci. Technol.* **2010,** *44* (16), 6054-6061.
10. Ng, D.-Q.; Strathmann, T. J.; Lin, Y.-P., Role of orthophosphate as a corrosion inhibitor in chloraminated solutions containing tetravalent lead corrosion product PbO_2. *Environ. Sci. Technol.* **2012,** *46* (20), 11062-11069.
11. Triantafyllidou, S.; Schock, M. R.; DeSantis, M. K.; White, C., Low contribution of PbO_2-coated lead service lines to water lead contamination at the tap. *Environ. Sci. Technol.* **2015,** *49* (6), 3746-3754.
12. EPA, U. S., Maximum contaminant level goals and national primary drinking water regulations for lead and copper. **1987**, 263–269.
13. Edition, F., Guidelines for drinking-water quality. *WHO chronicle* **2011,** *38* (4), 104-8.
14. Olson, T. M.; Wax, M.; Yonts, J.; Heidecorn, K.; Haig, S.-J.; Yeoman, D.; Hayes, Z.; Raskin, L.; Ellis, B. R., Forensic estimates of lead release from lead service lines during the Water Crisis in Flint, Michigan. *Environ. Sci. Tech. Let.* **2017,** *4* (9), 356-361.
15. Pieper, K. J.; Tang, M.; Edwards, M. A., Flint water crisis caused by interrupted corrosion control: Investigating “ground zero” home. *Environ. Sci. Technol.* **2017,** *51* (4), 2007-2014.
16. Edwards, M.; Dudi, A., role of chlorine and chloramine in corrosion of lead-bearing plumbing materials. *J. Am. Water. Works. Ass.* **2004,** *96* (10), 69-81.

17. Renner, R., Plumbing the depths of DC's drinking water crisis. *Environ. Sci. Technol.* **2004,** *38* (12), 224A-227A.

18. American Water Works Association (AWWA)., 2017 Water Utility Disinfection Survey Report. **2018**. https://www.awwa.org/2017DisinfectionSurveyReport.pdf

19. Liu, H.; Korshin, G. V.; Ferguson, J. F.; Jiang, W., Key parameters and kinetics of oxidation of lead (II) solid phases by chlorine in drinking water. *Water Pract. Tech.* **2006,** *1* (4).

20. Pan, W.; Pan, C.; Bae, Y.; Giammar, D., Role of Manganese in Accelerating the Oxidation of Pb (II) Carbonate Solids to Pb(IV) Oxide at Drinking Water Conditions. *Environ. Sci. Technol.* **2019,** *53* (12), 6699-6707.

21. DeSantis, M. K.; Triantafyllidou, S.; Schock, M. R.; Lytle, D. A., Mineralogical evidence of galvanic corrosion in drinking water lead pipe joints. *Environ. Sci. Technol.* **2018,** *52* (6), 3365-3374.

22. Masters, S.; Welter, G. J.; Edwards, M., Seasonal variations in lead release to potable water. *Environ. Sci. Technol.* **2016,** *50* (10), 5269-5277.

23. Lytle, D. A.; Schock, M. R., Formation of Pb (IV) oxides in chlorinated water. *Journal-American Water Works Association* **2005,** *97* (11), 102-114.

24. Tully, J.; DeSantis, M. K.; Schock, M. R., Water quality–pipe deposit relationships in Midwestern lead pipes. *AWWA Water Science* **2019,** *1* (2), e1127.

25. Bae, Y.; Pasteris, J. D.; Giammar, D. E., Impact of orthophosphate on lead release from pipe scale in high pH, low alkalinity water. *Water Research* **2020**, 115764.

26. Rego, C.; Schock, M. In *Discovery of unforeseen lead level optimization issues for high pH and low DIC conditions*, Water Quality and Technology Conference, Charlotte, NC, November, **2007**.

27. Colling, J.; Whincup, P.; Hayes, C., The measurement of plumbosolvency propensity to guide the control of lead in tapwaters. *Water Environ. J.* **1987,** *1* (3), 263-269.

28. Hopwood, J. D.; Derrick, G. R.; Brown, D. R.; Newman, C. D.; Haley, J.; Kershaw, R.; Collinge, M., The identification and synthesis of lead apatite minerals formed in lead water pipes. *J. Chem.* **2016,** 2016 (11p), 1-11.

29. Bae, Y.; Pasteris, J. D.; Giammar, D. E., The Ability of Phosphate To Prevent Lead Release from Pipe Scale When Switching from Free Chlorine to Monochloramine. *Environ. Sci. Technol.* **2020**, 54 (2), 879-888.

30. Lytle, D. A.; Schock, M. R., Formation of Pb(IV) oxides in chlorinated water. *J. Am. Water. Works. Ass.* **2005,** *97* (11), 102-114.

31. Liu, H.; Korshin, G. V.; Ferguson, J. F., Investigation of the kinetics and mechanisms of the oxidation of cerussite and hydrocerussite by chlorine. *Environ. Sci. Technol.* **2008,** *42* (9), 3241-3247.

32. Schock, M.; Giani, R., Oxidant/disinfectant chemistry and impacts on lead corrosion. *Proc. 2004 AWWA WQTC, San Antonio, Texas* **2004**.

33. Schock, M.; Harmon, S.; Swertfeger, J.; Lohmann, R. In Tetravalent lead: a hitherto unrecognized control of tap water lead contamination, *Water Quality Technology Conference, American Water Works Association* Nashville, TN: 2001; pp 2270-2291.

34. McNeill, L. S.; Edwards, M., Importance of Pb and Cu particulate species for corrosion control. *Environ. Eng.* **2004,** *130* (2), 136-144.

35. Davidson, C.; Peters, N.; Britton, A.; Brady, L.; Gardiner, P.; Lewis, B., Surface analysis and depth profiling of corrosion products formed in lead pipes used to supply low alkalinity drinking water. *Water Sci. and Technol.* **2004,** *49* (2), 49-54.

36. Mosseri, S.; Henglein, A.; Janata, E., Trivalent lead as an intermediate in the oxidation of lead (II) and the reduction of lead (IV) species. *J. Phy. Chem.* **1990,** *94* (6), 2722-2726.

37. Liu, H.; Kuznetsov, A. M.; Masliy, A. N.; Ferguson, J. F.; Korshin, G. V., Formation of Pb (III) intermediates in the electrochemically controlled Pb(II)/PbO_2 system. *Environ. Sci. Technol.* **2012,** *46* (3), 1430-1438.

38. Vasquez, F. A.; Heaviside, R.; Tang, Z.; Taylor, J. S., Effect of free chlorine and chloramines on lead release in a distribution system. *J. Am. Water. Works. Ass.* **2006,** *98* (2), 144-154.

39. Rajasekharan, V. V.; Clark, B. N.; Boonsalee, S.; Switzer, J. A., Electrochemistry of free chlorine and monochloramine and its relevance to the presence of Pb in drinking water. *Environ. Sci. Technol.* **2007,** *41* (12), 4252-4257.

40. Wang, Y.; Xie, Y.; Li, W.; Wang, Z.; Giammar, D. E., Formation of lead (IV) oxides from lead (II) compounds. *Environ. Sci. Technol.* **2010,** *44* (23), 8950-8956.

41. Schock, M. R.; Gardels, M. C., Plumbosolvency reduction by high pH and low carbonate—solubility relationships. *J. Am. Water. Works. Ass.* **1983,** *75* (2), 87-91.

42. Taylor, J.; Dietz, J.; Randall, A.; Hong, S., Impact of RO-desalted water on distribution water qualities. *Water Sci. Technol.* **2005,** *51* (6-7), 285-291.

43. McTigue, N. E.; Cornwell, D. A.; Graf, K.; Brown, R., Occurrence and consequences of increased bromide in drinking water sources. *J. Am. Water. Works. Ass.* **2014,** *106* (11), E492-E508.

44. Allard, S.; Fouche, L.; Dick, J.; Heitz, A.; Von Gunten, U., Oxidation of manganese (II) during chlorination: role of bromide. *Environ. Sci. Technol.* **2013,** *47* (15), 8716-8723.

45. Orta, J.; Patton, S.; Liu, H., Bromide-assisted catalytic oxidation of lead(II) solids by chlorine in drinking water distribution systems. *Chem. Commun.* **2017,** *53* (62), 8695-8698.

46. Zhu, Y.; Zhu, Z.; Zhao, X.; Liang, Y.; Huang, Y., Characterization, dissolution, and solubility of lead hydroxypyromorphite [$Pb_5(PO_4)_3OH$] at 25–45° C. *J. Chem* **2015,** 17(2), 1-10.

47. Jolley, R. L.; Carpenter, J. H. Aqueous chemistry of chlorine: chemistry, analysis, and environmental fate of reactive oxidant species; Oak Ridge National Lab., TN (USA): 1982.

48. Chebeir, M.; Liu, H., Kinetics and mechanisms of Cr(VI) formation via the oxidation of Cr(III) solid phases by chlorine in drinking water. *Environ. Sci. Technol.* **2016,** *50* (2), 701-710.

49. Rice, E. W.; Baird, R. B.; Eaton, A. D.; Clesceri, L. S., Standard methods for the examination of water and wastewater. American Public Health Association Washington, DC: 2012; Vol. 10.
50. Ravel, B.; Newville, M., Athena, Artemis, Hephaestus: data analysis for X-ray absorption spectroscopy using IFEFFIT. *J. Synchrotron Radiat.* **2005,** *12* (4), 537-541.
51. Bethke, C. M., Geochemical and biogeochemical reaction modeling. Cambridge University Press: **2007**.
52. Gustafsson, J., Visual MINTEQ ver. 3.1. JP Gustafasson, KTH, Sweden. **2015**.
53. Boffardi, B., Lead corrosion. *Journal of New England Water Works Association* **1995,** *109* (2), 121-131.
54. Johnson, B.; Yorton, R.; Tran, T.; Kim, J., Evaluation of corrosion control alternatives to meet the lead and copper rule for Eastern Massachusetts. **1993**.
55. Schock, M. R., Understanding corrosion control strategies for lead. *J. Am. Water. Works. Ass.* **1989,** *81* (7), 88-100.
56. Tang, Z.; Hong, S.; Xiao, W.; Taylor, J., Impacts of blending ground, surface, and saline waters on lead release in drinking water distribution systems. *Water Res.* **2006,** *40* (5), 943-950.
57. Boyd, G. R.; Dewis, K. M.; Korshin, G. V.; Reiber, S. H.; Schock, M. R.; Sandvig, A. M.; Giani, R., Effects of changing disinfectants on lead and copper release. *J. Am. Water. Works. Ass.* **2008,** *100* (11), 75-87.
58. Duranceau, S. J.; Lintereur, P. A.; Taylor, J. S., Effects of orthophosphate corrosion inhibitor on lead in blended water quality environments. *Desalin. Water Treat.* **2010,** *13* (1-3), 348-355.
59. Zhang, P.; Ryan, J. A., Transformation of Pb (II) from cerrusite to chloropyromorphite in the presence of hydroxyapatite under varying conditions of pH. *Environ. Sci. Technol.* **1999**, 33 (4), 625-630.
60. Peng, C.-Y.; Korshin, G. V.; Valentine, R. L.; Hill, A. S.; Friedman, M. J.; Reiber, S. H., Characterization of elemental and structural composition of corrosion scales and deposits formed in drinking water distribution systems. *Water Res.* **2010**, 44 (15), 4570-4580.
61. Schock, M. R.; Scheckel, K. G.; DeSantis, M.; Gerke, T. L., Mode of occurrence, treatment, and monitoring significance of tetravalent lead. *Proc. 2005 AWWA WQTC, Quebec City, Quebec* **2005**.
62. Triantafyllidou, S.; Parks, J.; Edwards, M., Lead particles in potable water. *J. Am. Water. Works. Ass.* **2007,** *99* (6), 107-117.
63. Korshin, G.; Liu, H., Preventing the colloidal dispersion of Pb (iv) corrosion scales and lead release in drinking water distribution systems. *Environ. Sci. Water Res. Technol.* **2019**, 5(7) 1262-1269.

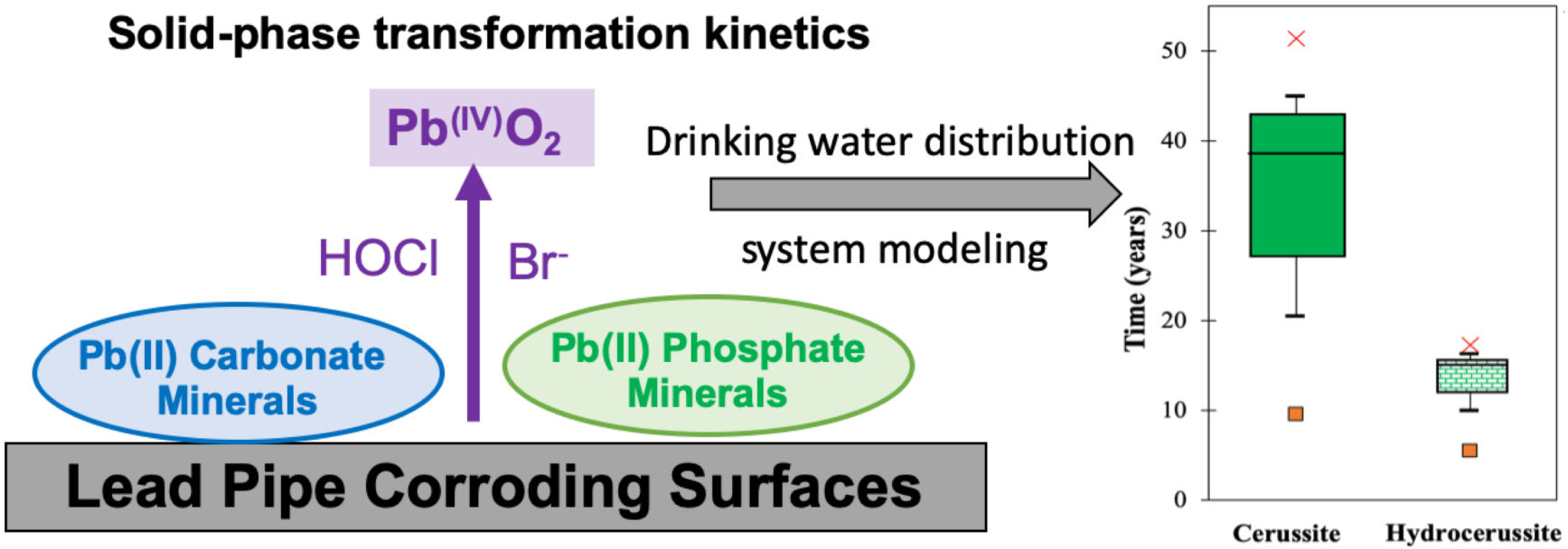
Solid-phase transformation kinetics
$Pb^{(IV)}O_2$
HOCl
Br^-
Pb(II) Carbonate Minerals
Pb(II) Phosphate Minerals
Lead Pipe Corroding Surfaces
Drinking water distribution system modeling
Time (years)
0
10
20
30
40
50
Cerussite
Hydrocerussite